

Article

Distinct Climate Effects on Dahurian Larch Growth at an Asian Temperate-Boreal Forest Ecotone and Nearby Boreal Sites

Enzai Du ^{1,2,*}  and Yang Tang ²

¹ State Key Laboratory of Earth Surface Processes and Resource Ecology, Faculty of Geographical Science, Beijing Normal University, Beijing 100875, China

² School of Natural Resources, Faculty of Geographical Science, Beijing Normal University, Beijing 100875, China

* Correspondence: enzaidu@bnu.edu.cn; Tel.: +86-010-5880-8085

Abstract: Climate change is exerting profound impacts on the structure and function of global boreal forest. Compared with their northern counterparts, trees growing at the southern boreal forest and the temperate-boreal forest ecotone likely show distinct responses to climate change. Based on annual basal areal increment (BAI) of Dahurian larch (*Larix gmelinii* Rupr.) plantations with similar ages, tree densities and soil nutrient conditions, we investigated the tree growth responses to inter-annual climate variations at an Asian temperate-boreal forest ecotone and nearby boreal sites in northeast China. Annual BAI changed nonlinearly with cambial age in the form of a lognormal curve. The maximum annual BAI showed no significant difference between the two bioregions, while annual BAI peaked at an elder age at the boreal-temperate forest ecotone. After eliminating the age associated trend, conditional regression analyses indicate that residual BAI at the boreal sites increased significantly with higher growing-season mean nighttime minimum temperature and non-growing-season precipitation, but decreased significantly with higher growing-season mean daytime maximum temperature during the past three decades (1985–2015). In contrast, residual BAI at the boreal-temperate forest ecotone only showed a positive and weak response to inter-annual variations of growing-season precipitation. These findings suggest distinct effects of inter-annual climate variation on the growth of boreal trees at the temperate-boreal forest ecotone in comparison to the southern boreal regions, and highlight future efforts to elucidate the key factors that regulate the growth of the southernmost boreal trees.

Keywords: boreal forest; boreal-temperate forest ecotone; basal area increment; climate change; inter-annual variation



Citation: Du, E.; Tang, Y. Distinct Climate Effects on Dahurian Larch Growth at an Asian Temperate-Boreal Forest Ecotone and Nearby Boreal Sites. *Forests* **2022**, *13*, 27. <https://doi.org/10.3390/f13010027>

Academic Editor: Craig Nitschke

Received: 22 November 2021

Accepted: 23 December 2021

Published: 26 December 2021

Publisher's Note: MDPI stays neutral with regard to jurisdictional claims in published maps and institutional affiliations.



Copyright: © 2021 by the authors. Licensee MDPI, Basel, Switzerland. This article is an open access article distributed under the terms and conditions of the Creative Commons Attribution (CC BY) license (<https://creativecommons.org/licenses/by/4.0/>).

1. Introduction

Boreal forest is experiencing strong climate change that results in profound impacts on tree growth and ecosystem function [1–4]. Climate warming has been found to alleviate the limitation of cold temperature and favor tree growth in some northern boreal forests [5,6]. Compared with its northern counterpart, southern boreal forest is theoretically less limited by cold temperature and likely shows a different response to climate change [4,7]. The southernmost boreal trees growing at the boreal-temperate forest ecotone may even respond negatively to climate warming due to an exceedance of the optimal growth temperature [8]. In addition, moisture stress is predicted to aggravate under warmer climate and may suppress tree growth in southern boreal forest [4]. These effects may jointly result in a decline in the dominance of boreal trees and thus a poleward shift of the southern boreal boundaries over time [1,9]. Understanding the climate effects on the growth of the southernmost boreal trees has important implications for the projection of future boreal forest dynamics, whereas relevant studies at the boreal-temperate forest ecotone are rare in literature [8,10].

The occurrence of climate warming is diurnally and seasonally uneven, likely resulting in diurnally and seasonally uneven effects on tree growth [11–13]. Experimental studies

have indicated that daytime warming can stimulate leaf photosynthesis and tree growth, while the effect may shift to neutral or even negative when the optimal temperature is exceeded and/or other factors (e.g., water availability) become more limiting [7,14,15]. In contrast, elevated nighttime temperature has been found to increase nighttime plant respiration and leaf photosynthesis during the following day through a reduction in carbohydrate feedback inhibition [11,16]. Moreover, warmer growing-season temperature favors tree growth in northern boreal forest that is limited by cold temperature but the effect can shift to be negative in southern boreal forest [17–20]. In contrast, climate warming during the non-growing season affects spring phenology and thereby tree growth during the following growing season [12]. However, the diurnally and seasonally uneven effects of temperature on boreal tree growth have rarely been tested at the boreal-temperate forest ecotone as compared with common boreal regions.

The effect of precipitation on tree growth also shows remarkable seasonality. More growing-season precipitation generally benefits tree growth in moisture limited regions [7,21]. In addition, trees can adjust physiologically in response to the moisture stress and rising atmospheric CO₂ concentrations, showing improved water use efficiency as indicated by changes in tree ring $\delta^{13}\text{C}$ values [22,23]. During the non-growing season, experimental reduction of snow cover in temperate and southern boreal forests has been found to decline tree growth in the following growing season mainly due to increased soil freezing injury of root systems and decreased water sources for tree growth at the beginning of the growing season [24,25]. Similarly, large-scale studies based on satellite data and/or tree ring data indicated a positive effect of winter snow on vegetation and/or tree growth during subsequent growing season, but this effect varied with climate condition [26,27]. In contrast, the increase of winter precipitation has been found to delay snow melt and reduce tree growth at the Siberian boreal forest–tundra ecotone [28]. Moreover, frosts at the start of the growing season could cause freezing injury and consequently decline tree growth [29]. Overall, precipitation during the growing season and non-growing season likely exerts significant but distinct effects on boreal tree growth in the boreal-temperate forest ecotone in comparison to common boreal regions.

Boreal forest in the Greater Khingan Mountains, northeast China, represents the southernmost edge of Asian taiga [30]. It shifts into temperate broadleaved forests in the southeast due to an increase in temperature with lower altitudes, resulting in a boreal-temperate forest ecotone [31]. Large areas of the primary boreal forest have been logged before the 1990s and extensive plantations of Dahurian larch (*Larix gmelinii* Rupr.) have been established to promote forest regrowth [32]. These plantations provide an opportunity to test the growth response of boreal trees to climate change by sampling plots with similar tree densities and even tree ages. Well-designed studies of boreal tree growth across these plantations may avoid the intervention by varied strength of competition either between same species or among different species, the effect of which is difficult to tackle in natural forests [33,34].

By sampling tree ring cores from replicated Dahurian larch plantations at a temperate-boreal forest ecotone and adjacent boreal sites in northeast China, we explored the larch tree growth at these two bioregions and the responses to inter-annual variation of six temperature associated variables and four moisture associated variables (see Section 2.4 for detailed information). Specifically, we tested the following hypotheses: (1) the response of larch tree growth to temperature and precipitation is seasonally and diurnally uneven; (2) larch tree growth at the boreal-temperate forest ecotone is not responsive to inter-annual temperature variation, while growing-season temperature controls larch tree growth at the boreal sites; (3) larch tree growth at the boreal-temperate forest ecotone is limited by growing-season precipitation, while at the boreal sites non-growing season precipitation mediated tree growth during the following growing season.

2. Materials and Methods

2.1. Study Areas

Boreal forest in the Greater Khingan Mountains consists of large areas of Dahurian larch with companion tree species like white birch (*Betula platyphylla* Sukaczew.) and Chinese aspen (*Populus davidiana* Dode.). Along with a shift in climate conditions in the southeast, there exists a boreal-temperate forest ecotone, being characterized by a mixture of Dahurian larch and Mongolian oak (*Quercus mongolica* Fisch. ex Ledeb.). In the Greater Khingan Mountains, logging activities before the 1990s have resulted in large areas of secondary forests and Dahurian larch plantations, which are of relatively young ages [32]. This study was conducted in Dahurian larch plantations at a boreal-temperate forest ecotone and adjacent boreal sites (Figure 1; Table 1). The annual mean temperature (MAT) increased from -3.3 °C at the boreal sites to -0.1 °C at the boreal-temperate forest ecotone (Table 1). Mean annual precipitation (MAP) was higher at the boreal-temperate forest ecotone (551 vs. 445 mm), while the aridity index indicated lower humidity at the boreal-temperate forest ecotone (Table 1).

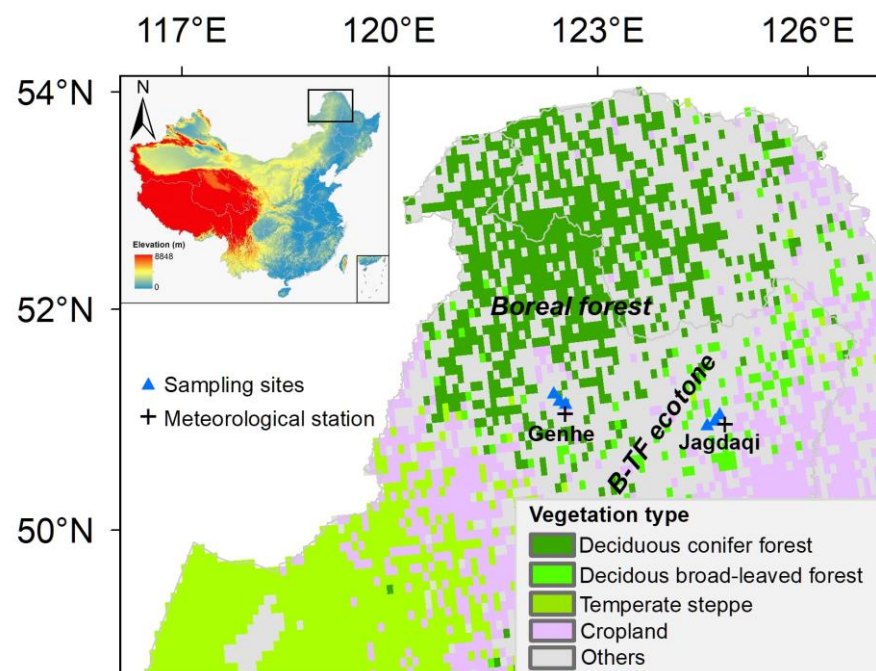


Figure 1. Locations of the sampled Dahurian larch plantations at the boreal sites and the boreal-temperate forest ecotone in northeast China.

Table 1. General information on the sampled Dahurian larch plantations at the boreal sites and the boreal-temperate forest ecotone. Note that stand age was estimated as the cambial age at the breast height. Aridity index (AI) was estimated as the ratio between mean annual precipitation (MAP) and mean annual temperature (MAT) plus ten Celsius [35]. The abbreviation DBH indicates the diameter at breast height.

	Stand ID	Latitude (°E)	Longitude (°N)	Elevation (m)	MAT (°C)	MAP (mm)	AI	Mean DBH (cm)	Mean Height (m)	Stand Age (year)
Boreal site	Stand 1	120.71	50.44	804	-3.3	445	66	24.4 ± 1.6	14.8 ± 1.1	35
	Stand 2	120.84	50.49	815	-3.3	445	66	21.8 ± 1.2	16.2 ± 0.7	35
	Stand 3	120.96	50.41	797	-3.3	445	66	23.2 ± 3.1	17.1 ± 0.8	32
Boreal-temperate forest ecotone	Stand 4	123.95	50.42	407	-0.1	551	56	29.0 ± 2.9	16.2 ± 1.0	38
	Stand 5	124.06	50.45	403	-0.1	551	56	28.6 ± 2.8	16.4 ± 0.3	40
	Stand 6	124.15	50.49	408	-0.1	551	56	28.6 ± 3.1	15.7 ± 0.8	40

2.2. Field Sampling

Field sampling was conducted during late August in 2016. Three replicated Dahurian larch plantations, located at relatively flat slopes ($<5^\circ$), were sampled at the boreal-temperate forest ecotone and the boreal sites, respectively (Figure 1). The cambial age of sampled plantations at the boreal-temperate forest ecotone and the boreal sites was 38–40 and 32–35 years, respectively (Table 1). The tree height was similar (14.8–17.1 vs. 15.7–16.4 m) at both bioregions, and the diameter at breast height was significantly larger for the sampled plantations at the boreal-temperate forest ecotone (28.6–29.0 vs. 21.8–24.4 cm, $p < 0.05$) (Table 1).

In view of the fact that trees in each sampled plantation were even-aged and evenly planted, a small number of sampled trees can reasonably represent the growth of each plantation stand. In order to save labor cost and avoid potential injuries to many trees, six trees were randomly selected in each plantation stand and tree ring cores were sampled using an increment borer (5.15 mm internal diameter; Haglöf Sweden, Långsele, Sweden) in two opposite directions (i.e., south–north and east–west) at the breast height (1.3 m above the ground). In total, 72 cores from 36 trees were sampled and all samples contained the innermost tree rings. In each stand, DBH was measured for each tree using a diameter tape. Tree height was measured using an Ultrasound Height Distance Measuring Instrument (Vertex IV, Haglof, Sweden).

Five soil subsamples were randomly collected for the 0–10 cm soil layer using an auger in each plantation stand. Undecomposed litters on the surface were removed before soil sampling. Soil subsamples in each plantation stand were mixed as a composite sample. Nutrient concentrations of soil samples were further measured in the laboratory.

2.3. Laboratory Measurements

Tree-ring samples were air dried under room temperature, fixed in wooden holders and carefully sanded. Tree ring widths were measured with a precision of 0.001 mm using a LINTAB 5.0 system (RINNTECH, Heidelberg, Germany). The time-series of tree ring width were cross-dated visually and corrected using the COFECHA program [36]. Cross-dated tree ring width chronologies are shown in the Supplementary Information (Figure S1). Soil samples were air-dried and sieved through a 2 mm mesh to remove gravel and coarse plant debris. Fine root fragments were removed by handpicking. Soil available P was extracted using 0.5 mol L⁻¹ NaHCO₃ solution at pH 8.5 and measured by a colorimetric method using an ultraviolet visible spectrophotometer (UV-2550, UV-Visible Spectrophotometer, Shimadzu, Japan). Soil samples were further ground using an agate mortar grinder (NM200, Retsch, Haan, Germany) and sieved through a 100-mesh sieve. Alkali-hydrolyzable N concentration was determined using an alkali-hydrolysis and diffusion method. Soil total N concentration was analyzed using an Elementar Vario EL Cube (Elementar Analysis system GmbH, Hanau, Germany). After an acid digestion with a mixture of nitric, perchloric and hydrofluoric acids, concentrations of total phosphorus (P), potassium (K), calcium (Ca) and magnesium (Mg) were measured using an inductively coupled plasma optical emission spectrometer (Optima 5300 DV, PerkinElmer, Waltham, MA, USA).

2.4. Data on Phenology and Climate Variables

Understanding the phenological phases is important to define key climate variables that potentially regulate plant growth. Field observations in the study areas found that leaf expansion of Dahurian larch mainly occurred in May and leaf senescence occurred mainly in September [37]. To test the potential shifts in the timing of phenological phases over the period 1985–2015, we estimated the start and end of the growing season (the day-of-years at which the NDVI curvature reached maximum value) by fitting a double logistic function to the smoothed and snow-corrected time series of the third generation Global Inventory Monitoring and Modeling System NDVI Index (GIMMS NDVI3g, <https://ecocast.arc.nasa.gov/data/pub/gimms/>, accessed on 21 November 2021) [38]. In line with the field observations, the satellite-derived start and end of the growing season

occurred in May and September, respectively (Figures S2 and S3). Although previous studies indicate that the start and end of the growing season can shift over time as driven by climate warming [39,40], no such trends were found in our study areas over the past three decades (Figures S2 and S3). Therefore, this study defined May and September as the beginning and ending months of the growing season, respectively.

Monthly climate data during 1985–2015 were derived from two meteorological stations (accessed from China Meteorological Data Service Center, <http://data.cma.cn>, accessed on 21 November 2021) adjacent to the sampled plantations (Gehen Station for the boreal sites; Jagdaqi Station for the boreal-temperate forest ecotone) (Figure 1). Six temperature associated variables and four moisture associated variables were calculated for further analysis. Specifically, temperature associated variables included mean temperature for the beginning month (i.e., May) and ending month of growing season (i.e., September) [37], mean daytime maximum temperature and nighttime minimum temperature of the growing season, mean daytime maximum temperature and nighttime minimum temperature of non-growing season. The moisture associated variables included precipitation of the beginning month (i.e., May) and ending month of the growing season (i.e., September) [39], growing-season precipitation, and non-growing-season precipitation.

2.5. Calculation of Annual Basal Area Increment

The two ring width series were first averaged for each tree. Considering that trees in each plantation stand were even-aged, tree ring widths of the six trees were further averaged to derive a composite time series to indicate the overall tree growth in each stand. In this study, stand age was estimated as the cambial age at the breast height based on the total tree ring numbers. Annual basal area increments (BAI, $\text{cm}^2 \text{yr}^{-1}$) were calculated based on the composite time series of tree ring data following Equation (1),

$$\text{BAI} = \pi(R_n^2 - R_{n-1}^2) \quad (1)$$

where R_n and R_{n-1} represent the tree radius at the stand age of n and $n - 1$ years, respectively. Compared with tree ring width, annual basal area increment is a better indicator of tree growth and productivity, especially at relatively young ages [41,42]. For instance, the same tree ring width of different ages does not necessarily mean the same amount of biomass accumulation in view of an increase in DBH with elder tree age. Considering that the sampled plantations were at relatively young ages (32–40 years, see Table 1 for more details), BAIs were used for further statistical analysis of Dahurian larch growth and its response to inter-annual climate variations.

2.6. Statistical Analysis

The temporal changes of BAI along with tree age (yr) fitted well to a lognormal curve as Equation (2)

$$\text{BAI} = \text{BAI}_{\max} * \frac{1}{e^{0.5 * (\frac{\ln \text{age} - \ln \text{age}_0}{b})^2}} \quad (2)$$

where BAI_{\max} , b , and age_0 are parameters. Specifically, BAI_{\max} indicates the maxima of BAI and age_0 indicates the age that BAI approaches the maxima. Student's t -test was used to test the difference of the maximum annual BAI and the age that annual BAI approaches the maxima between boreal-temperate forest ecotone and the boreal sites. BAIs of each plantation stand were thus detrended using the lognormal curve to remove the age-associated trend in tree growth. Residual BAIs were used for further analysis of the climate effects on larch tree growth.

To identify the effects of climate variables on residual BAIs, we used the 'glmulti' package to conduct a model selection analysis of the six temperature associated variables and four moisture associated variables based on Akaike's information criterion with a correction for small sample sizes (AICc) [43,44]. The relative importance of each climate variable was estimated as the sum of the Akaike weights for the models in which the

variable appeared. A cut-off relative importance value of 0.8 was used to differentiate between the important and unimportant variables [43]. The multicollinearity of the climate drivers included in the final model was evaluated using the variance inflation factor (VIF < 3 indicates weak collinearity) [45]. We conducted conditional regression analysis for each important climate variable to visualize its relationship with the residual BAI while holding all other variables constant [46]. The variance explained by each climate variable was further estimated by averaging sequential sums of squares over all orderings of regressors [47]. All statistical analyses were performed using R software (version 3.6.3) with a significance level of $p < 0.05$ [48].

3. Results

3.1. Climate Trends and Soil Nutrients in the Two Bioregions

The inter-annual variations of temperature and precipitation associated variables both were seasonally asymmetric, showing distinct trends in the growing season, non-growing season, and the beginning and ending months of the growing season (Figures S4–S6). During the past three decades (1985–2015), growing-season temperature showed a significant increase both at the southern boreal sites ($p < 0.01$, Figure S4a,c) and the boreal-temperate forest ecotone ($p < 0.05$, Figure S4b,d), while no significant warming trend was found in other seasons (Figures S4e–h and S5). Precipitation generally showed no significant trends (Figure S6a–d,g,h), except an increase in the starting month of the growing season (May) ($p < 0.001$, Figure S6e,f). Soil concentrations of N, P, K, Ca and Mg showed no significant difference between the sampled plantation stands at the boreal sites and the boreal-temperate forest ecotone (Table S1).

3.2. Changes of Annual Basal Area Increment with Tree Age

Our results indicate an intrinsic growth curve of Dahurian larch trees both at the boreal-temperate forest ecotone and boreal sites. Specifically, the temporal changes of annual BAI with stand age were in line with a lognormal curve (Figure 2; Table 2). Tree age explained 53%~68% and 39%~59% of the temporal variation in annual BAI at the boreal-temperate forest ecotone and the boreal sites, respectively (Table 2). The maximum annual BAI at the boreal-temperate forest ecotone ($16.0 \pm 1.3 \text{ cm}^2 \text{ yr}^{-1}$) showed no significant difference from that at the boreal sites ($13.1 \pm 2.5 \text{ cm}^2 \text{ yr}^{-1}$) (Student's *t* test, $p = 0.11$). However, annual BAI at the boreal-temperate forest ecotone approached a peak at an elder cambial age ($16.6 \pm 1.6 \text{ yr}$) than that at the boreal sites ($12.0 \pm 1.3 \text{ yr}$) (Student's *t*-test, $p = 0.03$). When eliminating the trend associated with stand age, residual BAI showed no significant trends over past three decades (1985–2015) both at the boreal-temperate forest ecotone ($p = 0.79$) and boreal sites ($p = 0.56$) (Figure 3).

3.3. Climate Regulation of Tree Growth in Past Three Decades

Our analysis showed a seasonally and diurnally uneven climate regulation of residual BAI at the boreal sites (total variance explained 47%, $p < 0.001$; Table S2). Specifically, residual BAI was mainly explained by inter-annual variations of mean daytime maximum temperature, mean nighttime minimum temperature during the growing season, and precipitation during the non-growing season (Figure 4a). Conditional regression analysis showed that residual BAI increased significantly with mean nighttime minimum temperature during the growing season (variance explained 21.5%, $p < 0.001$; Figure 4b) and precipitation during the last non-growing season (variance explained 6.8%, $p < 0.001$; Figure 4d), while it decreased significantly with mean daytime maximum temperature during the growing season (variance explained 18.7%, $p < 0.001$; Figure 4c). At the boreal-temperate forest ecotone, climate showed distinct effects on residual BAI. Specifically, residual BAI increased significantly with growing-season precipitation (variance explained 9.2%, $p = 0.003$; Figure 5b, Table S3). In line with our hypothesis, residual BAI at the boreal-temperate forest ecotone was not responsive to inter-annual variations of temperature associated variables (Figure 5a).

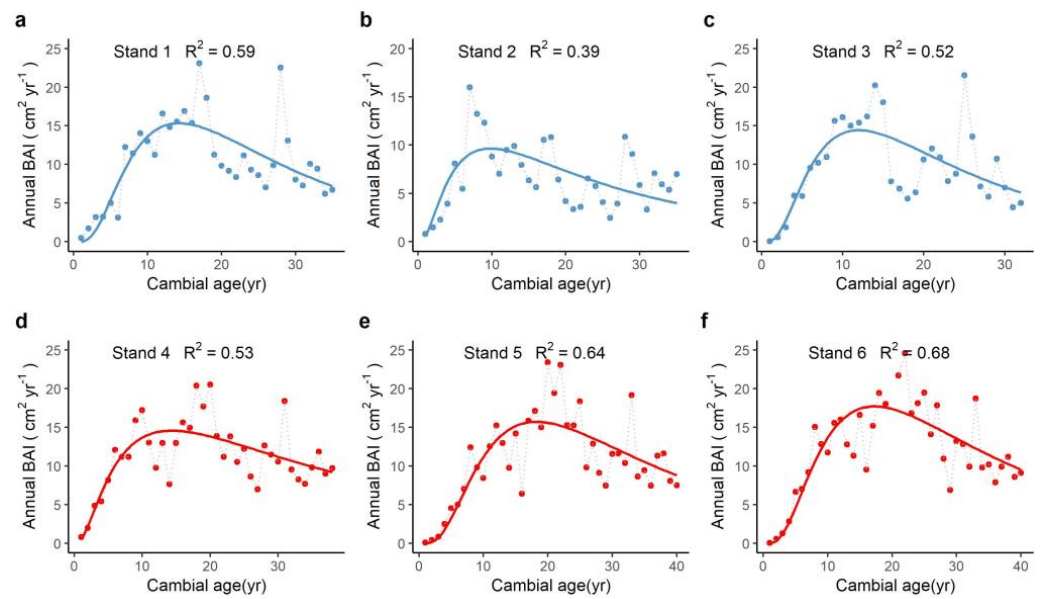


Figure 2. Changes in mean annual basal area increment (BAI, $\text{cm}^2 \text{yr}^{-1}$) with cambial age (yr) at breast height for the six Dahurian larch plantations at the boreal sites (a–c) and the boreal-temperate forest ecotone (d–f) in northeast China.

Table 2. A summary of the annual BAI-age curve fitting for the six sampled Dahurian larch plantations. The symbol *** indicates a significance at $p < 0.001$. Numbers in the brackets indicate the standard errors of estimated coefficients.

Location	Stand ID	BAI _{max}	b	Age ₀	R ²
Boreal site	Stand 1	15.3(1.1) ***	0.73(0.09) ***	14.3(1.0) ***	0.59
	Stand 2	9.7(0.9) ***	0.96(0.14) ***	9.8(1.2) ***	0.39
	Stand 3	14.4(1.3) ***	0.77(0.11) ***	12.0(1.0) ***	0.52
Boreal-temperate forest ecotone	Stand 4	14.6(0.8) ***	1.01(0.12) ***	14.4(1.2) ***	0.56
	Stand 5	15.7(1.0) ***	0.73(0.08) ***	18.2(1.1) ***	0.64
	Stand 6	17.7(1.0) ***	0.76(0.08) ***	17.2(0.9) ***	0.68

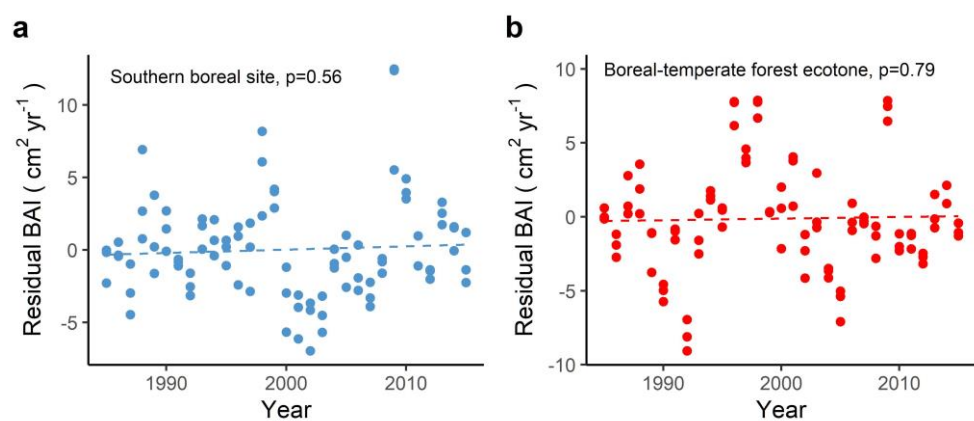


Figure 3. Temporal variation of residual BAI of Dahurian larch plantations during 1985–2015 at the boreal sites (a) and the boreal-temperate forest ecotone (b) in northeast China.

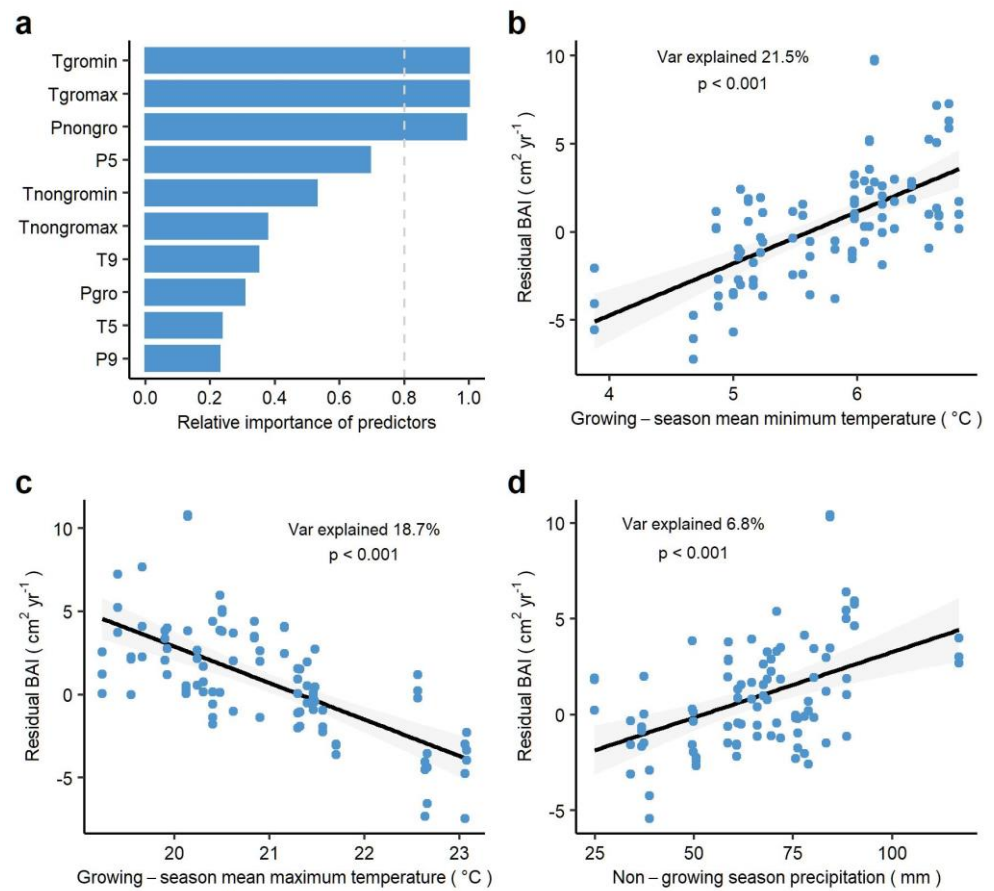


Figure 4. Relative importance of ten climatic variables that potentially regulate the temporal variation in residual BAI (a) and conditional regression plots showing the relationship between residual BAI and each important regulator at the boreal sites (b–d). Abbreviations: Tgromax, mean daytime maximum temperature during growing season; Tgromin, mean nighttime minimum temperature during growing season; Tnongromax, mean daytime maximum temperature during the last nongrowing season; Tnongromin, mean nighttime minimum temperature during the last nongrowing season; T5, mean temperature in May; T9, mean temperature in September; Pgro, growing-season precipitation; Pnongro, non-growing-season precipitation; P5, precipitation in May; P9, precipitation in September.

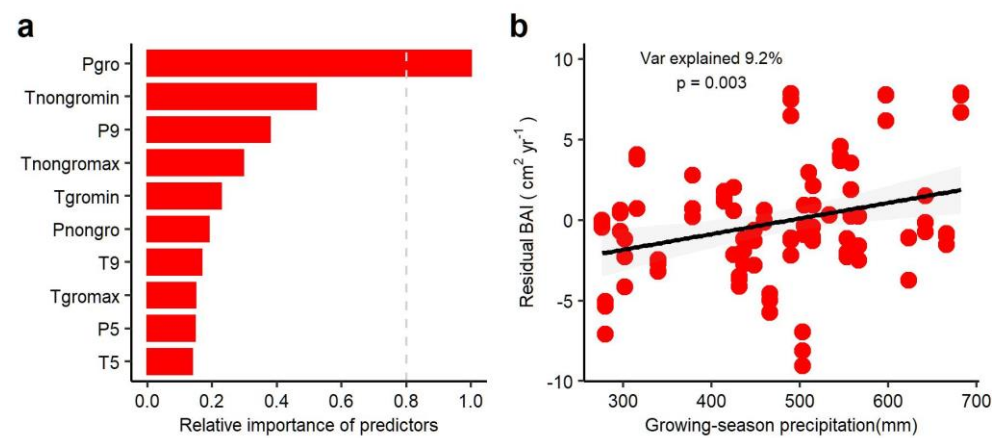


Figure 5. Relative importance of ten climatic variables that potentially regulate the temporal variation in residual BAI (a) and the relationship between residual BAI and growing-season precipitation at the boreal-temperate forest ecotone (b). See the caption of Figure 4 for the abbreviations.

4. Discussion

4.1. Responses of Tree Growth to Inter-Annual Variation in Temperature

In line with our hypothesis, the growth response of the Dahurian larch tree to inter-annual variation in temperature was seasonally and diurnally asymmetric. Residual BAI showed a significant response to inter-annual variation of growing-season temperatures at the boreal sites, while no significant role of temperature associated variables was found during other periods (e.g., the non-growing season, the start and end months of the growing season) (Figure 4a), implying that climate warming at the non-growing season likely exert limited effects on tree growth in the southern boreal region. Different from the counterparts at the boreal sites, the annual growth of Dahurian larch at the boreal-temperate forest ecotone was not responsive to all temperature associated variables (Figure 5a). This implies that a relatively warmer climate at the boreal-temperate forest ecotone has likely alleviated the temperature limitation of the Dahurian larch at its southern distribution limit.

Intriguingly, the annual growth of Dahurian larch showed significant and opposite responses to growing-season daytime and nighttime temperatures at the boreal sites (Figure 4a,c). Residual BAI showed a negative response to inter-annual variation of growing-season daytime maximum temperature (generally > 20 °C; Figure S4a), being likely due to the fact that growing-season daytime maximum temperature had exceeded the optimal temperature for gross primary productivity of deciduous conifers (ranging 15–20 °C) [49]. However, residual BAI showed a positive response to inter-annual variation of nighttime temperature during the growing season in the southernmost boreal forests, being in line with the experimental results showing that higher nighttime temperature stimulated leaf photosynthesis during the following day through a reduction in carbohydrate feedback inhibition [11,16]. In contrast to our results, an analysis using satellite-derived normalized difference vegetation index suggested a positive response of vegetation growth to growing-season daytime maximum temperature, and a negative response to nighttime minimum temperature in northern boreal regions [50]. Our findings highlight that the diurnally asymmetric effects of daytime and nighttime temperatures are likely distinct in the southern boreal forests compared with their northern counterparts.

4.2. Responses of Tree Growth to Inter-Annual Variations in Precipitation

In line with our hypothesis, the results indicate distinct growth responses of Dahurian larch to the precipitation associated variables at the boreal-temperate forest ecotone and the boreal sites. Specifically, residual BAI showed a positive response to non-growing-season precipitation (being mainly snowfall below zero °C as shown by Figure S4) at the boreal sites. This result generally agrees with the experimental findings that the manipulated reduction of snow cover during the non-growing season resulted in a strong decline of tree growth during the following growing season [24,25]. The positive effects of non-growing-season snow on tree growth are likely due to two causes. First, the reduction of snowpack generally increases soil freezing and causes root damage that consequently reduces water and nutrient uptake capacity in the following growing season, thereby suppressing the tree growth [24,51,52]. Additionally, thinner winter snowpack also limits water sources for tree growth at the beginning of the growing season during which water inputs from precipitation are usually low and frequently occur in the form of frost [53,54]. In contrast, growing-season precipitation significantly constrained the growth of Dahurian larch at the boreal-temperate forest ecotone but not at the boreal sites. This difference might be due to the fact that the climate at the boreal-temperate forest ecotone showed a higher aridity than the southern boreal sites, as indicated by lower values of aridity index (Table 1).

4.3. Uncertainties and Future Research Needs

Tree growth is simultaneously regulated by biotic and abiotic factors, such as competition among species or individuals, soil nutrient conditions, and climate variables. Based on well-designed sampling across Dahurian larch plantations with relatively comparable conditions of stand age, tree intensity and soil nutrients, we explored the climate effects

on inter-annual tree growth variations. Different from plantations, natural forests are characterized by an uneven age structure and strong species competition [55]. The tree growth-climate response of natural forests may differ from that found in plantations.

Growing-season precipitation only explained a low proportion (9.2%) of the inter-annual variation in Dahurian larch growth at the boreal-temperate forest ecotone and other climate variables were found to be unimportant, highlighting more research efforts to understand the key regulators of boreal tree growth at the boreal-temperate forest ecotone. In view of an increase in evapotranspiration caused by future climate warming, boreal trees will likely be subject to increasing risk of moisture deficiency in the southernmost boreal forests [25,56]. As driven by a rise of atmospheric CO₂ concentration, the improvement of water use efficiency may partially alleviate the moisture stress in the boreal-temperate forest ecotone [57], but this benefit seems unable to compensate the overall negative effects from water deficiency. In that case, Dahurian larch at the boreal-temperate forest ecotone will likely decline in performance and potentially be competed out by temperate trees (e.g., Mongolian oak) that are favored by warmer temperatures, resulting in a northward shift in the southern boundary of Asian boreal forest [2,9]. Further research efforts are thus needed to elucidate the ecophysiological adaptation of boreal tree species and consequent ecological (e.g., species composition) and biogeochemical (e.g., carbon and nitrogen cycling) changes in these southernmost boreal forests.

5. Conclusions

Using data on annual BAI of Dahurian larch plantations with similar cambial ages, tree densities, and soil nutrient conditions, we investigated the tree growth characteristics and their responses to inter-annual climate variations at a temperate-boreal forest ecotone and nearby boreal sites in northeast China. The results demonstrated that annual BAI changed nonlinearly with tree age in the form of a lognormal curve, supporting a new approach to eliminate the age associated trend in tree growth. Further analyses suggest distinct climate effects on the larch tree growth between the two bioregions. Residual BAI at the southern boreal sites responded positively to growing-season mean nighttime minimum temperature and non-growing-season precipitation, and was negatively influenced by growing-season mean daytime maximum temperature, while larch tree growth at the boreal-temperate forest ecotone was only limited by growing-season precipitation. These findings improve the current understanding of the climate effects on the growth of the southernmost boreal trees and have important implications for the projection of future boreal forest dynamics.

Supplementary Materials: The following are available online at <https://www.mdpi.com/article/10.3390/f13010027/s1>, Figure S1: Temporal variations of crossdated tree ring width (mm yr⁻¹) for the six Dahurian larch plantations at the southern boreal sites (a–c for stands 1–3) and the boreal-temperate forest ecotone (d–f for stands 4–6), Figure S2: Three-decadal variations in satellite-derived beginning dates of growing season for the six Dahurian larch plantations at the southern boreal sites (a–c for stands 1–3) and the boreal-temperate forest ecotone (d–f for stands 4–6), Figure S3: Three-decadal variations in satellite-derived ending dates of growing season for the six Dahurian larch plantations at the southern boreal sites (a–c for stands 1–3) and the boreal-temperate forest ecotone (d–f for stand 4–6), Figure S4: Three-decadal variations (1985–2015) of growing-season mean daytime maximum temperature (a,b), growing-season mean nighttime minimum temperature(c,d), non-growing-season mean daytime maximum temperature (e,f), and non-growing-season mean night minimum temperature (g,h) at the southern boreal sites and the boreal-temperate forest ecotone, Figure S5: Three-decadal variations (1985–2015) of monthly mean temperature in May (a,b) and September (c,d) at the southern boreal sites and the boreal-temperate forest ecotone, Figure S6: Three-decadal variations (1985–2015) of growing-season precipitation (a,b), non-growing-season precipitation (c,d), monthly precipitation in May (e,f) and September (g,h) at the southern boreal sites and the boreal-temperate forest ecotone, Table S1: Soil nutrient concentrations of sampled Dahurian larch plantations at the southern boreal sites and the boreal-temperate forest ecotone. Values are shown as mean ± standard deviation, Table S2: A summary of the model for the residual BAI of Dahurian larch at the southern boreal sites using growing-season mean nighttime minimum temperature (Tgromin),

growing-season mean daytime maximum temperature (Tgromax), and non-growing-season precipitation (Pnongro) as important regulators (residual BAI~Tgromin + Tgromax + Pnongro). Variance inflation factors for Tgromin, Tgromax and Pnongro were 1.21, 1.45 and 1.22, respectively, implying inconsiderable collinearity among regulators, Table S3: A summary of the model for the residual BAI of Dahurian larch at the boreal-temperate forest ecotone using growing season precipitation (Pgro) as the important regulator (residual BAI~Pgro).

Author Contributions: Conceptualization, E.D.; methodology, E.D.; validation, E.D. and Y.T.; formal analysis, E.D.; investigation, E.D.; writing—original draft preparation, E.D.; writing—review and editing, E.D. and Y.T.; funding acquisition, E.D. All authors have read and agreed to the published version of the manuscript.

Funding: This research was funded by the National Natural Science Foundation of China (41630750 and 41877328) and the State Key Laboratory of Earth Surface Processes and Resource Ecology (2021-TS-02).

Institutional Review Board Statement: Not available.

Informed Consent Statement: Not available.

Data Availability Statement: Not available.

Acknowledgments: The authors are grateful to Longchao Xu, Aujun Xing and Wenqing Li for their assistance in field and laboratory work.

Conflicts of Interest: The authors declare no conflict of interest.

References

1. Chapin, F.; Callaghan, T.; Bergeron, Y.; Fukuda, M.; Johnstone, J.; Juday, G.; Zimov, S. Global change and the boreal forest: Thresholds, shifting states or gradual change? *AMBIO J. Hum. Environ.* **2004**, *33*, 361–365. [[CrossRef](#)]
2. Soja, A.; Tchebakova, N.; French, N.; Flannign, M.; Shugart, H.; Stocks, B.; Sukhinin, A.; Parfenova, E.; Chapin, F.; Stackhouse, P. Climate-induced boreal forest change: Predictions versus current observations. *Glob. Planet. Change* **2007**, *56*, 274–296. [[CrossRef](#)]
3. Beck, P.; Juday, G.; Alix, C.; Barber, V.; Winslow, S.; Sousa, E.; Goetz, S. Changes in forest productivity across Alaska consistent with biome shift. *Ecol. Lett.* **2011**, *14*, 373–379. [[CrossRef](#)] [[PubMed](#)]
4. Lloyd, A.; Bunn, A.; Berner, L. Latitudinal gradient in tree growth response to climate warming in the Siberian taiga. *Glob. Chang. Biol.* **2011**, *17*, 1935–1945. [[CrossRef](#)]
5. Sherriff, R.; Miller, A.; Muth, K.; Schriver, M.; Batzel, R. Spruce growth responses to warming vary by ecoregion and ecosystem type near the forest-tundra boundary in south-west Alaska. *J. Biogeogr.* **2017**, *44*, 1457–1468. [[CrossRef](#)]
6. Zhu, Z.; Piao, S.; Myneni, R.; Huang, M.; Zeng, Z.; Canadell, J.; Ciais, P.; Sitch, S.; Friedlingstein, P.; Arneeth, A. Greening of the Earth and its drivers. *Nat. Clim. Chang.* **2016**, *6*, 791–795. [[CrossRef](#)]
7. D’Orangeville, L.; Houle, D.; Duchesne, L.; Phillips, R.P.; Bergeron, Y.; Kneeshaw, D. Beneficial effects of climate warming on boreal tree growth may be transitory. *Nat. Commun.* **2018**, *9*, 3213. [[CrossRef](#)]
8. Frelich, L.; Montgomery, R.; Reich, P. Seven ways a warming climate can kill the southern boreal forest. *Forests* **2021**, *12*, 560. [[CrossRef](#)]
9. Fisicelli, N.; Frelich, L.; Reich, P. Temperate tree expansion into adjacent boreal forest patches facilitated by warmer temperatures. *Ecography* **2014**, *37*, 152–161. [[CrossRef](#)]
10. Evans, P.; Brown, C. The boreal–temperate forest ecotone response to climate change. *Environ. Rev.* **2017**, *25*, 423–431. [[CrossRef](#)]
11. Turnbull, M.; Murthy, R.; Griffin, K. The relative impacts of daytime and night-time warming on photosynthetic capacity in *Populus deltoides*. *Plant Cell Environ.* **2002**, *25*, 1729–1737. [[CrossRef](#)]
12. Xia, J.; Chen, J.; Piao, S.; Ciais, P.; Luo, Y.; & Wan, S. Terrestrial carbon cycle affected by non-uniform climate warming. *Nat. Geosci.* **2014**, *7*, 173–180. [[CrossRef](#)]
13. Tan, J.; Piao, S.; Chen, A.; Zeng, Z.; Ciais, P.; Janssens, I.; Vicca, S. Seasonally different response of photosynthetic activity to daytime and night-time warming in the Northern Hemisphere. *Glob. Chang. Biol.* **2015**, *21*, 377–387. [[CrossRef](#)] [[PubMed](#)]
14. Walker, X.; Johnstone, J. Widespread negative correlations between black spruce growth and temperature across topographic moisture gradients in the boreal forest. *Environ. Res. Lett.* **2014**, *9*, 064016. [[CrossRef](#)]
15. Kumarathunge, D.; Drake, J.; Tjoelker, M.; López, R.; Pfautsch, S.; Vårhammar, A.; Medlyn, B. The temperature optima for tree seedling photosynthesis and growth depend on water inputs. *Glob. Chang. Biol.* **2020**, *26*, 2544–2560. [[CrossRef](#)]
16. Turnbull, M.; Tissue, D.; Murthy, R.; Wang, X.; Sparrow, A.; Griffin, K.L. Nocturnal warming increases photosynthesis at elevated CO₂ partial pressure in *Populus deltoides*. *N. Phytol.* **2004**, *161*, 819–826. [[CrossRef](#)]
17. Jarvis, P.; Linder, S. Constraints to growth of boreal forests. *Nature* **2004**, *405*, 904–905. [[CrossRef](#)]
18. Reich, P.; Sendall, K.; Stefanski, A.; Rich, R.; Hobbie, S.E.; Montgomery, R.A. Effects of climate warming on photosynthesis in boreal tree species depend on soil moisture. *Nature* **2000**, *562*, 263–267. [[CrossRef](#)]

19. Jiang, Y.; Zhang, J.; Han, S.; Chen, Z.; Setälä, H.; Yu, J.; Zheng, X.; Guo, Y.; Gu, Y. Radial growth response of *Larix gmelinii* to climate along a latitudinal gradient in the Greater Khingan Mountains, Northeastern China. *Forests* **2016**, *7*, 295. [CrossRef]
20. Li, W.; Jiang, Y.; Dong, M.; Du, E.; Zhou, Z.; Zhao, S.; Xu, H. Diverse responses of radial growth to climate across the southern part of the Asian boreal forests in northeast China. *For. Ecol. Manag.* **2020**, *458*, 117759. [CrossRef]
21. Hynes, A.; Hamann, A. Moisture deficits limit growth of white spruce in the west-central boreal forest of North America. *For. Ecol. Manag.* **2020**, *461*, 117944. [CrossRef]
22. Walker, X.; Mack, M.; Johnstone, J. Stable carbon isotope analysis reveals widespread drought stress in boreal black spruce forests. *Glob. Chang. Biol.* **2015**, *21*, 3102–3113. [CrossRef] [PubMed]
23. Keenan, T.; Hollinger, D.; Bohrer, G.; Dragoni, D.; Munger, J.; Schmid, H.; Richardson, A. Increase in forest water-use efficiency as atmospheric carbon dioxide concentrations rise. *Nature* **2013**, *499*, 324–327. [CrossRef] [PubMed]
24. Blume-Werry, G.; Kreyling, J.; Laudon, H.; Milbau, A. Short-term climate change manipulation effects do not scale up to long-term legacies: Effects of an absent snow cover on boreal forest plants. *J. Ecol.* **2016**, *104*, 1638–1648. [CrossRef]
25. Reinmann, A.; Susser, J.; Demaria, E.; Templer, P. Declines in northern forest tree growth following snowpack decline and soil freezing. *Glob. Chang. Biol.* **2019**, *25*, 420–430. [CrossRef] [PubMed]
26. Peng, S.; Piao, S.; Ciais, P.; Fang, J.; Wang, X. Change in winter snow depth and its impacts on vegetation in China. *Glob. Chang. Biol.* **2010**, *16*, 3004–3013. [CrossRef]
27. Wu, X.; Li, X.; Liu, H.; Ciais, P.; Li, Y.; Xu, C.; Babst, F.; Guo, W.; Hao, B.; Wang, P.; et al. Uneven winter snow influence on tree growth across temperate China. *Glob. Chang. Biol.* **2019**, *25*, 144–154. [CrossRef] [PubMed]
28. Vaganov, E.; Hughes, M.; Kirilyanov, A.; Schweingruber, F.; Silkin, P. Influence of snowfall and melt timing on tree growth in subarctic Eurasia. *Nature* **1999**, *400*, 149–151. [CrossRef]
29. Hänninen, H. Climate warming and the risk of frost damage to boreal forest trees: Identification of critical ecophysiological traits. *Tree Physiol.* **2006**, *26*, 889–898. [CrossRef] [PubMed]
30. Shugart, H.; Shugart, H.; Leemans, R.; Bonan, G. *A Systems Analysis of the Global Boreal Forest*; Cambridge University Press: Cambridge, UK, 1992; pp. 1–10.
31. Su, Y.; Guo, Q.; Hu, T.; Guan, H.; Jin, S.; An, S.; Ma, K. An updated vegetation map of China (1:1000,000). *Sci. Bull.* **2020**, *65*, 1125–1136. [CrossRef]
32. Tian, H.; Xu, H.; Hall, A.S. Pattern and change of a boreal forest landscape in northern China. *Water Air Soil Pollut.* **1995**, *82*, 465–476. [CrossRef]
33. Coomes, D.; Allen, R. Effects of size, competition and altitude on tree growth. *J. Ecol.* **2007**, *95*, 1084–1097. [CrossRef]
34. Forrester, D. Linking forest growth with stand structure: Tree size inequality, tree growth or resource partitioning and the asymmetry of competition. *For. Ecol. Manag.* **2019**, *447*, 139–157. [CrossRef]
35. De Martonne, E. Aerisme, et indices d'aridité. *Comptesrendus L'Academie Sci.* **1926**, *182*, 1395–1398.
36. Holmes, R. Computer-assisted quality control in tree-ring dating and measurement. *Tree-Ring Bull.* **1983**, *43*, 69–78.
37. Du, E.; Fang, J. Linking belowground and aboveground phenology in two boreal forests in Northeast China. *Oecologia* **2014**, *176*, 883–892. [CrossRef]
38. Beck, P.; Atzberger, C.; Høgda, K.; Johansen, B.; Skidmore, A. Improved monitoring of vegetation dynamics at very high latitudes: A new method using MODIS NDVI. *Remote Sens. Environ.* **2006**, *100*, 321–334. [CrossRef]
39. Yang, B.; He, M.; Shishov, V.; Tychkov, I.; Vaganov, E.; Rossi, S.; Ljungqvist, F.; Bräuning, A.; Griesinger, J. New perspective on spring vegetation phenology and global climate change based on Tibetan Plateau tree-ring data. *Proc. Natl. Acad. Sci. USA* **2017**, *114*, 6966–6971. [CrossRef]
40. Rosbakh, S.; Hartig, F.; Sandanov, D.V.; Bukharova, E.V.; Miller, T.K.; Primack, R.B. Siberian plants shift their phenology in response to climate change. *Glob. Chang. Biol.* **2021**, *27*, 4435–4448. [CrossRef]
41. Babst, F.; Bouriaud, O.; Alexander, R.; Trouet, V.; Frank, D. Toward consistent measurements of carbon accumulation: A multi-site assessment of biomass and basal area increment across Europe. *Dendrochronologia* **2014**, *32*, 153–161. [CrossRef]
42. Fu, L.; Sharma, R.; Zhu, G.; Li, H.; Hong, L.; Guo, H.; Duan, G.; Shen, C.; Lei, Y.; Li, Y.; et al. A basal area increment-based approach of site productivity evaluation for multi-aged and mixed forests. *Forests* **2017**, *8*, 119. [CrossRef]
43. Calcagno, V.; de Mazancourt, C. glmulti: An R package for easy automated model selection with (generalized) linear models. *J. Stat. Softw.* **2010**, *34*, 1–29. [CrossRef]
44. Burnham, K.; & Anderson, D. Multimodel Inference: Understanding AIC and BIC in Model Selection. *Sociol. Methods Res.* **2004**, *33*, 261–304. [CrossRef]
45. Zuur, A.; Ieno, E.; Elphick, C. A protocol for data exploration to avoid common statistical problems. *Methods Ecol. Evol.* **2010**, *1*, 3–14. [CrossRef]
46. Breheny, P.; Burchett, W. Visualization of regression models using visreg. *R J.* **2013**, *9*, 56–71. [CrossRef]
47. Grömping, U. Relative importance for linear regression in R: The package relaimpo. *J. Stat. Softw.* **2006**, *17*, 1–27. [CrossRef]
48. R Development Core Team. R Foundation for Statistical Computing. Vienna, Austria. Available online: <https://www.r-project.org/> (accessed on 1 December 2020).
49. Huang, M.; Piao, S.; Ciais, P.; Peñuelas, J.; Wang, X.; Keenan, T.; Janssens, I. Air temperature optima of vegetation productivity across global biomes. *Nat. Ecol. Evol.* **2019**, *3*, 772–779. [CrossRef]

50. Peng, S.; Piao, S.; Ciais, P.; Myneni, R.; Chen, A.; Chevallier, F.; Zeng, H. Asymmetric effects of daytime and night-time warming on Northern Hemisphere vegetation. *Nature* **2013**, *501*, 88–92. [[CrossRef](#)]
51. Wipf, S.; Rixen, C. A review of snow manipulation experiments in Arctic and alpine tundra ecosystems. *Polar Res.* **2010**, *29*, 95–109. [[CrossRef](#)]
52. Harrison, J.; Blagden, M.; Green, M.; Salvucci, G.; Templer, P.H. Water sources for red maple trees in a northern hardwood forest under a changing climate. *Ecohydrology* **2020**, *13*, e2248. [[CrossRef](#)]
53. Ffolliott, P.; Gottfried, G.; Baker, M.B., Jr. Water yield from forest snowpack management: Research findings in Arizona and New Mexico. *Water Resour. Res.* **1989**, *25*, 1999–2007. [[CrossRef](#)]
54. Langs, L.; Petrone, R.; Pomeroy, J. A $\delta^{18}\text{O}$ and $\delta^2\text{H}$ stable water isotope analysis of subalpine forest water sources under seasonal and hydrological stress in the Canadian Rocky Mountains. *Hydrol. Processes* **2020**, *34*, 5642–5658. [[CrossRef](#)]
55. Carle, J.; Vuorinen, P.; Del Lungo, A. Status and trends in global forest plantation development. *For. Prod. J.* **2002**, *52*, 12–23.
56. Naumann, G.; Alfieri, L.; Wyser, K.; Mentaschi, L.; Betts, R.A.; Carrao, H.; Feyen, L. Global changes in drought conditions under different levels of warming. *Geophys. Res. Lett.* **2018**, *45*, 3285–3296. [[CrossRef](#)]
57. Keeling, R.; Graven, H.; Welp, L.; Resplandy, L.; Bi, J.; Piper, S.; Meijer, H. Atmospheric evidence for a global secular increase in carbon isotopic discrimination of land photosynthesis. *Proc. Natl. Acad. Sci. USA* **2017**, *114*, 10361–10366. [[CrossRef](#)] [[PubMed](#)]